Stop-band type NGD RLC-resonant circuit sensitivity analysis

Eric Jean Roy Sambatra[1], Fayrouz Haddad[2], Samuel Ngoho[3], Mathieu Guerin[2], Wenceslas Rahajandraibe[2], Habachi Bilal[2], Glauco Fontgalland[4], Hugerles S. Silva[5,6], and Blaise Ravelo[7]

[1]Institut Supérieur de Technologie (IST-D), BP 509, Antsiranana 201, Madagascar
[2]Aix-Marseille University, CNRS, University of Toulon, IM2NP UMR7334, Marseille, France
[3]Association Française de Science des Systèmes (AFSCET), 151 Bd de l'Hôpital, Paris 75013, France
[4]University of Mount Union, School of Engineering, 906 S. Union Ave, Alliance, OH, 44601, USA
[5]Instituto de Telecomunicações and Departamento de Eletrónica, Telecomunicações e Informática, Universidade de Aveiro, Campus Universitário de Santiago, 3810-193 Aveiro, Portugal
[6]Department of Electric Engineering, University of Brasília (UnB), Brasilia, 70910-900, Brazil
[7]Nanjing University of Information Science & Technology, School of Electronic & Information Engineering Nanjing, China 210044

Corresponding author: gerard-habachi.bilal@univ-amu.fr.

ABSTRACT This paper investigates on the rarely studied negative group delay (NGD) RF circuit with innovative stop-band (SB) behavior. In difference with the classical filter, the SB-NGD function is identified in function of frequency bands where the group delay (GD) presents negative sign. The ideal diagram specifying the SB-NGD function is introduced by indicating all the appropriate parameters. The S-parameter analytical model of the circuit is established. The SB-NGD analysis is developed. The main specifications of the SB-NGD circuit are expressed in function of its constituting components. Then, the design synthesis equations enabling to determine the SB-NGD circuit in function of the desired specifications as the center frequency and GD are built up. To illustrate concretely the feasibility of the SB-NGD function, a circuit proof-of-concept composed of LC-series network is theoretically analyzed. A parametric analysis on the SB circuit elements is accomplished to appraise the influence of each element on the SB-NGD specifications. To validate the unfamiliar SB-NGD theory, a prototype is fabricated and tested. The GD measured response of the considered circuit is compared by simulations and analytical calculations. SB-NGD responses showing a good agreement between the calculation and simulation are obtained with a 15 MHz center frequency, 44 ns GD and 3 MHz bandwidth.

INDEX TERMS Circuit theory, negative group delay (NGD) topology, RLC-network, Stop-band (SB) NGD analysis, SB-NGD synthesis, SB-NGD design, S-matrix modelling.

I. INTRODUCTION

THE negative group delay (NGD) theory and design is one of most intriguing and unfamiliar research topics in RF engineering nowadays. Tentative of tremendous applications of NGD circuits notably in the area of radio frequency (RF) and microwave engineering [1-13]. However, compared to other electronic and communication functions as antenna, filter, amplifier, modulator, mixer, phase shifter and oscillator, the NGD function requires more research works especially in academic area to be familiar to all electronic engineers. A review synthesis of some NGD applications is reported in [1]. Thanks to the NGD function, different applications as:

- An efficient technique of group delay (GD) compensation by considering the algebraic addition of positive and negative delays was developed [2-4].
- The technique was also exploited to the RF and microwave signal integrity especially for the improvement of distortion [5, 6].
- The combination of positive GD and NGD circuits was an innovative technique for designing RF and microwave phase shifters [7, 8].
- A very promising future application of NGD circuit for the phase array antenna in order to reduce the delay effect was proposed in [9, 10].
- An innovative application of NGD circuit to realize non-Foster reactive elements was also proposed [11]. Based on this technique, a design technique of negative capacitance was introduced [12].
- And very recent research about the application of tri-

band NGD circuit for wireless system was presented [13].

Nevertheless, many of RF, microwave and electronics engineers have further questions because of non-familiarity to NGD function. Therefore, a state of the art about the most fundamental NGD circuit theory is necessary. Thanks to the natural analytical relation between the refractive index and group velocity, it was also investigated that the negative group index optical media are equivalent to the possibility or propagate pulse waves under negative group velocity [14-15]. By taking into account the physical length of the media, the possibility of pulse signal propagating with NGD within a coaxial photonic crystal was demonstrated [16]. The concept of negative refractive index was democratized in early 2000s thanks to the revolution of metamaterials [17-19]. These artificial materials are expected to exhibit both negative permittivity and negative permeability [17-19]. The metamaterial passive structures are also known to operate with left-handed properties [19] which is the inverse of well-know and familiar right-handed property associated to electromagnetic (EM) wave propagation in natural media as transmission line (TL). Thanks to the use of particular structures as split ring resonator (SRR) [18], RF and microwave NGD passive circuits were designed. It was also found that there is a possibility to design NGD circuits with resistive lossy left-handed TLs [19]. Nonetheless, most of metamaterial circuits operate with NGD effect under significant losses. Therefore, new research direction was open to design low-loss and compact NGD passive circuits [21-26]. The best solution of low-loss and compact effects is the design of distributed NGD passive circuits with TLs [21-24]. Then, evolutive design of NGD circuits with tunable center frequency property was successfully developed [22]. To avoid loss effect, active NGD circuit was also proposed [27]. It can be understood at this state of bibliographic study that the NGD circuits can be designed with different structures. Reaching this phase of NGD design understanding, many questions are still open especially about the fundamental NGD circuit. To answer to the curious question, a state of the art about the most fundamental NGD circuit theory is described in the follow paragraph.

Based on the consideration of transfer function magnitude and GD, it was underlined that there is an analogy between the filter theory and NGD theory [28-29]. The concept of low-pass (LP) [28-31], high-pass (HP) [28-29, 32-33], and even bandpass (BP) [28-29, 34-35], NGD functions are innovatively initiated. It is worth to emphasize that because of the NGD intriguing properties and our familiarity to the filter terminologies, we may confuse LP-filter and LP-NGD [28-31], HP-filter and HP-NGD [28-29, 32-33], and BP-filter and BP-NGD [28-29, 34-35] functions. The identification of these different types of NGD functions enables to classify in the simplest ways, all the NGD circuits. But at this stage, we may wonder about the main fundamental differences between the filter and NGD theory. As answer to that curious query, the filter circuit theory is based on the transmittance magnitude diagram, and however the NGD circuit response analysis is based on the GD diagram. Keeping this difference in mind, unfamiliar LP-NGD circuits with GD negative from 0 to the NGD cut-off frequencies were designed [28, 29-31]. Then, less familiar NGD circuits with HP-NGD behavior were designed [28-29, 32-33]. So far, the most of RF and microwave NGD circuits [32,34] were designed to operate as BP-NGD function.

The NGD circuit theory inspired from the filter one opens a huge research work in order to be familiarized with the specialist. We can emphasize that the majority of papers published about the NGD circuit engineering [1-27] are focused on either LP- or BP- type NGD functions. So far, many curious questions rising from NGD researchers about the design method of stop-band (SB) type NGD circuits. For example, we may curiously ask about the feasibility of SB-NGD circuit design. This curious query motivates us to study the SB-NGD circuit design method in this paper whose outline will be presented in the next subsection.

Despite the progress of research work on the NGD circuit design [1-31], so far, few investigations are available in the literature on the design of the class of SB NGD circuits [32, 36-37]. The present study is addressing the first SB-NGD circuit design by considering an LC-series network circuit. The paper is organized in the five main sections as follows:

- Section II describes the topological representation and S-matrix modelling of the SB-NGD circuit under study.
- Section III introduces the SB-NGD circuit theoretical analysis.
- Section IV investigates on the parametric analysis of SB-NGD circuit proof of concept (POC).
- Section V presents the prototyping and experimental validation results of the SB-NGD circuit.
- Then, Section VI is the final conclusion.

II. TOPOLOGICAL STUDY NECESSARY TO IDENTIFY THE SB-NGD CIRCUIT

The present section examines the S-matrix representation of two-port topology. The SB-NGD function specifications are defined.

A. S-MATRIX REPRESENTATION

Similar to most of RF and microwave circuits, the modelling of the SB-NGD ones is based on the consideration of the equivalent S-matrix. Fig. 1 represents the general block diagram of a two-port circuit.

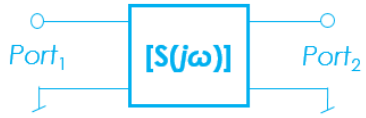

FIGURE 1. Two-port S-parameters black box.

By considering the angular frequency variable $j\omega$, the S-parameter model can be analytically defined by the 2-D matrix:

$$[S(j\omega)]=\begin{bmatrix} S_{11}(j\omega) & S_{12}(j\omega) \\ S_{21}(j\omega) & S_{22}(j\omega) \end{bmatrix} \quad (1)$$

In the case of a symmetrical passive circuit, this S-matrix can be reduced thanks to the following equality $S_{11}(j\omega)=S_{22}(j\omega)$ and $S_{12}(j\omega)=S_{21}(j\omega)$. Taking into account these equations, we can follow the frequency responses necessary for the SB-NGD analysis in the following subsection.

B. RECALL ON FREQUENCY RESPONSE PARAMETERS NECESSARY FOR THE SB-NGD STUDY

The main quantities necessary for the NGD analysis of RF and microwave circuits are the magnitude, phase and essentially the GD. The reflection and transmission magnitude coefficients are respectively defined by $S_{11}(\omega)=|S_{11}(j\omega)|$ and $S_{21}(\omega)=|S_{21}(j\omega)|$. The phase represents the argument of the transmission coefficient $\varphi(\omega)=\arg[S_{21}(j\omega)]$. And the NGD analysis must be obviously preceded by the GD expression which is defined by:

$$GD(\omega)=-\frac{\partial\varphi(\omega)}{\partial\omega}. \quad (2)$$

We emphasize that the GD represents the delay of propagation signal envelopes which can be physically understood from the group velocity.

C. SB-NGD FUNCTION SPECIFICATIONS

Similar to the filter theory, the NGD response is defined in function of the existence of frequency band where the GD previously expressed in equation (2) becomes negative $GD(\omega)<0$. Figs. 2 show the ideal graphical diagrams of the SB-NGD specifications, meanly the GD, the transmission and reflection coefficients. According to Fig. 2(a), the SB-NGD analysis is fundamentally linked to the determination of the circuit specifications as:

- i) The NGD cut-off frequencies $\omega_1=2\pi f_1$ and $\omega_2=2\pi f_2$ which are the roots of the GD:

$$GD(\omega)=0\Rightarrow\begin{cases} GD(\omega_1)=0 \\ GD(\omega_2)=0 \end{cases} \quad (3)$$

- ii) The NGD center frequency $\omega_0=2\pi f_0$,
- iii) The NGD bandwidth $\Delta\omega=2\pi\Delta f=\omega_2-\omega_1$ and the NGD value:

$$GD(\omega_0)=GD_0<0. \quad (4)$$

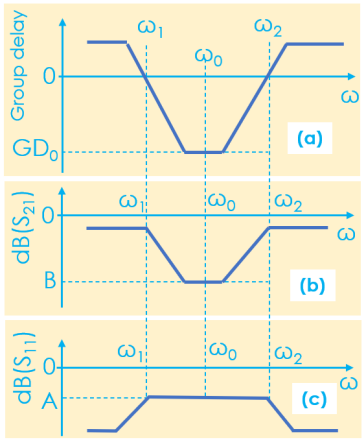

FIGURE 2. Ideal frequency responses of (a) GD, (b) reflection and (c) transmission coefficients of SB-NGD function.

Reflection and transmission coefficients can be respectively defined as:

$$S_{11}(\omega_0)=A<1 \quad (5)$$

$$S_{21}(\omega_0)=B<1. \quad (6)$$

D. DIFFERENCES BETWEEN THE CLASSICAL AND SB-NGD FUNCTION

It is worth to note that according to the regular filter theory, the VTF is essentially specified from the magnitude. However, the SB-NGD function is based on the exploration of GD. Table I summarizes the main differences between the SB-NGD and filter functions. The SB-NGD characteristics which will be explored in the remainder part of the paper can be understood from this table.

TABLE I. COMPARISON BETWEEN CLASSICAL BP FILTER AND SB-NGD FUNCTIONS

Parameters	Classic BP filter	SB-NGD function
Fundamental basis	Transmission coefficient magnitude	GD
Cut-off frequency	$\begin{cases} S_{21}(\omega_1)=\max[S_{21}(\omega)]/\sqrt{2} \\ S_{21}(\omega_2)=\max[S_{21}(\omega)]/\sqrt{2} \end{cases}$	Equation (3)
Center frequency	$S_{21}(\omega_0)=\max[S_{21}(\omega)]$	Equation (4)

Knowing the basic definition, the SB-NGD analysis of the LC-series network-based topology under study is theoretically investigated in the following section.

III. SB-NGD CIRCUIT ANALYSIS

The fundamental analysis of SB-NGD circuit is elaborated in the present section.

A. S-PARAMETER MODELING

Fig. 3 depicts the topology of the two-port passive and symmetric circuit under study. The considered topology is composed of series impedance constituted by a resistance in parallel with an LC-series network. We can denote the LC-

network equivalent admittance:

$$\zeta(j\omega)=\frac{jC\omega}{1-\omega^2/\omega_0^2} \tag{7}$$

with the resonance frequency which will be assumed as the center frequency off the SB-NGD response $\omega_0=1/\sqrt{LC}$.

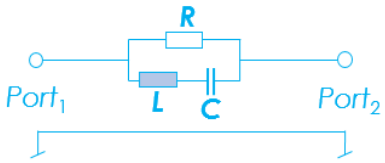

FIGURE 3. SB-NGD circuit under study.

Based on the circuit theory, we can demonstrate that the admittance matrix model of our circuit can be expressed by:

$$[Y(j\omega)]=\left(\frac{1}{R}+\zeta(j\omega)\right)\cdot\begin{bmatrix}1 & -1\\ -1 & 1\end{bmatrix}. \tag{8}$$

Based on the Y-to-S matrix transform [32], we have the corresponding S-matrix:

$$[S(j\omega)]=\left\{\begin{bmatrix}1 & 0\\ 0 & 1\end{bmatrix}-R_0[\zeta(j\omega)]\right\}\times\left\{\begin{bmatrix}1 & 0\\ 0 & 1\end{bmatrix}+R_0[\zeta(j\omega)]\right\}^{-1} \tag{9}$$

where R_0=50 Ω is the reference impedance. It is worth to note that R_0 represents the reference impedance associated to the S-parameter calculation. It is associated to the terminal charges and sources connected to Port1 and Port2 of the circuit under study. After exploitation of this relationship, we have the reflection and transmission coefficient analytical results, respectively:

$$S_{11}(j\omega)=\frac{R}{R+2R_0+2R_0R\zeta(j\omega)} \tag{10}$$

$$S_{21}(j\omega)=\frac{2R_0[1+R\zeta(j\omega)]}{R+2R_0+2R_0R\zeta(j\omega)}. \tag{11}$$

The frequency domain analysis proposed in subsection II-C leads to the following theoretical formulations.

B. S-PARAMETER MAGNITUDES

The magnitude of the reflection coefficient given in equation (10) is equal to:

$$S_{11}(\omega)=\frac{R}{\sqrt{rD_{11}^2(\omega)+iD_{11}^2(\omega)}} \tag{12}$$

where:

$$\begin{cases}rD_{11}(\omega)=(R-2R_0)(\omega_0^2-\omega^2)\\ iD_{11}(\omega)=2R_0RC\omega_0^2\omega\end{cases}. \tag{13}$$

The magnitude of the transmission coefficient proposed in equation (11) is written as:

$$S_{21}(\omega)=\frac{\sqrt{rN_{21}^2(\omega)+iN_{21}^2(\omega)}}{\sqrt{rD_{11}^2(\omega)+iD_{11}^2(\omega)}} \tag{14}$$

with:

$$\begin{cases}rN_{21}(\omega)=2R_0(\omega_0^2-\omega^2)\\ iN_{21}(\omega)=2R_0RC\omega_0^2\omega\end{cases}. \tag{15}$$

C. PHASE AND GD ANALYTICAL RESPONSES

From the transmission coefficient proposed in (11), one can express the transmission phase as:

$$\varphi(\omega)=\arctan\left(\frac{RC\omega_0^2\omega}{\omega_0^2-\omega^2}\right)-\arctan\left[\frac{2R_0RC\omega_0^2\omega}{(R-2R_0)(\omega_0^2-\omega^2)}\right] \tag{16}$$

The proposed circuit GD derived from this phase expression via equation (2):

$$GD(\omega)=\frac{R^2C\omega_0^2(\omega_0^2+\omega^2)(n_0+n_2\omega^2+n_4\omega^4)}{\left[(1+R^2C^2\omega^2)\omega_0^4+\omega^2(\omega^2-2\omega_0^2)\right](d_0+d_2\omega^2+d_4\omega^4)} \tag{17}$$

with:

$$\begin{cases}n_0=-R-2R_0\\ n_2=2\omega_0^2\left[R^2C^2R_0\omega_0^2+R+2R_0\right]\\ n_4=-\omega_0^4(R+2R_0)\\ d_0=(R+2R_0)^2\\ d_2=2\omega_0^2\left[2R^2C^2R_0^2\omega_0^2-(R+2R_0)^2\right]\\ d_4=\omega_0^4(R+2R_0)^2\end{cases} \tag{18}$$

It can be noticed that the GD expressed in (16) presents numerator and denominator expressions as polynomial quantities which may have a negative sign.

D. SB-NGD EXISTENCE CONDITIONS

The SB-NGD specifications are indicated by the ideal diagram in Fig. 2. Therefore, we can determine analytically each parameter of the SB-NGD response by considering the S-parameter and GD model established in the previous subsection. Substituting the resonance frequency, $\omega=\omega_0$ into the GD expressed in equation (17), we have:

$$GD(\omega_0)=\frac{1}{R_0C\omega_0^2}>0. \tag{19}$$

It can be notice that this GD is always positive for any parameters of the circuit shown in Fig. 3. In addition, it can be derived by substituting $\omega=\omega_0$ into the reflection and transmission coefficients given in equations (12) and (14) that $S_{11}(\omega_0)=0$ and $S_{21}(\omega_0)=1$. The roots of the GD written in equation (17) are:

$$\omega_1=\frac{\sqrt{\left[R^2C^2R_0\omega_0^2+R+2R_0\right]-\sqrt{\left[R^2C^2R_0\omega_0^2+R+2R_0\right]^2-4(R+2R_0)^2}}}{\omega_0\sqrt{(R+2R_0)}} \tag{20}$$

$$\omega_2 = \frac{\sqrt{\left[R^2C^2R_0\omega_0^2 + R + 2R_0\right] + \sqrt{\left[R^2C^2R_0\omega_0^2 + R + 2R_0\right]^2 - 4(R+2R_0)^2}}}{\omega_0\sqrt{(R+2R_0)}} \quad (21)$$

At the very low frequencies, the GD written in equation (17) becomes:

$$GD(\omega \approx 0) = \frac{-2R^2C}{R+2R_0}. \quad (22)$$

This GD is always negative whatever the parameters R, L and C of the circuit under study. To demonstrate that $GD(\omega > \omega_0)$ is negative, let us consider the angular frequency $\omega_n = n \cdot \omega_0$ with integer, n>2. Substituting the resonance frequency, $\omega = \omega_0$ into the GD expressed in equation (17), we have the expression of $GD_n = GD(n\omega_0)$ as follows:

$$GD_n = \frac{\left\{R^2C(n^2+1)\right\}}{\left\{\left[2R^2C^2n^2\omega_0^2 - (R+2R_0)(n^2+2)^2\right]\right\}} < 0. \quad (23)$$
$$\left\{\left[2R^2C^2n^2\omega_0^2 + (n-1)^2\right]\right\}$$
$$\left\{\left[4R^2C^2n^2\omega_0^2 + (R+2R_0)^2(n-2)^2\right]\right\}$$

The denominator of this last expression is always positive. However, the numerator can be positive when:

$$2R^2C^2n^2\omega_0^2 - (R+2R_0)(n^2+2)^2 \le 0. \quad (24)$$

In other words, this inequality can be rewritten as:

$$\left(n + \frac{2}{n}\right)^2 \ge \frac{2R^2C^2\omega_0^2}{R+2R_0}. \quad (25)$$

or

$$n^2 - \frac{RC\omega_0\sqrt{2}}{\sqrt{R+2R_0}}n + 2 \ge 0. \quad (26)$$

This means that when previous condition is satisfied, we have $GD_n \le 0$. This final analytical demonstration states that at certain higher frequencies, the GD of our circuit is unconditionally negative. The combination of equations (18), (22) and (26) enables to affirm that the circuit under study behaves theoretically as SB-NGD function.

E. SB-NGD DESIGN EQUATIONS

The SB-NGD circuit design can be performed in function of the desired center frequency, f_0, GD value, GD_0, reflection and transmission coefficients, and NGD bandwidth. By inverting the equation of the GD proposed in equation (19), we can determine the capacitor by the equation:

$$C = \frac{1}{R_0 GD_0 \omega_0^2} \quad (27)$$

From the resonance frequency equation, we have:

$$L = \frac{1}{C\omega_0^2} \quad (28)$$

At very low frequency ($\omega \approx 0$), the reflection coefficient proposed in equation (12) can be expressed as:

$$S_{11}(\omega \approx 0) = \frac{R}{R+2R_0} \quad (29)$$

By inverting the equation, S_{11}=A, from this last equation, we have:

$$R = \frac{2R_0A}{1-A} \quad (30)$$

To verify the feasibility of the developed SB-NGD theory, a synthesis of POC from expected specification will be analyzed in the following section.

IV. PARAMETRIC ANALYSIS OF SYNTHESIZED SB-NGD CIRCUIT

The feasibility of the SB-NGD circuit is introduced in the presented section by synthesizing a POC of lumped circuit. A sensitivity analysis is based on analytical calculation by sweeping the resistor, inductor and capacitor values. The calculated reflection and transmission coefficients, and GDs are performed by using MATLAB® from expressions (12), (14) and (17) respectively.

A. SYNTHESIS OF SB-NGD CIRCUIT POC

The relevance of the previously established S-parameter and GD models is verified by synthesizing the POC of the passive and ideal circuit introduced in Fig. 3. The POC was designed to have the desired specifications given in Table II which indicated the center frequency, GD and NGD bandwidth.

TABLE II. Desired specifications of the SB-NGD function

Designation	Name	Value
Centre frequency	f_c	15 MHz
GD	GD_0	44 ns
Matching level	A	A_a=-12 dB A_b=-10 dB
NGD	Δf	3 MHz

The calculations were carried out from previously established formulas (27), (28) and (30). The calculated values of R, L and C components constituting the SB-NGD circuit POC is addressed in Table III. The influence of the passive circuit components on the SB-NGD function can be understood from the parametric and sensitivity analysis. Each lumped RLC component varies on a defined range of values between +/-5%. The SB-NGD sensitivity study focuses on the analysis of the GD, the transmission and reflection parameters with respect to frequency.

TABLE II. Component values of the considered POC circuit

Nature	Name	Value
Resistor	R	R_a=33.5 Ω R_b=46.2 Ω
Inductor	L	2.2 µH
Capacitor	C	51.2 pF

The SB-NGD function parametric analysis results are elaborated in the next subsection.

B. PARAMETRIC ANALYSIS OF RESISTOR R=R_a

In this last case of sensitivity analysis, the influence of resistor R=R_a+/-5% from 31.825 Ω to 35.175 Ω on the SB-NGD response is investigated. Accordingly, Figs. 4 depict the computed results of cartographies versus (f, R). These mappings highlight how GD, S_{21} and S_{11} behaves under variation of resistive element R. It is particularly interesting to state here that the SB-NGD behavior is kept in the range of the resistive element variation. Then, we can underline that the center frequency does not change with the resistor variation.

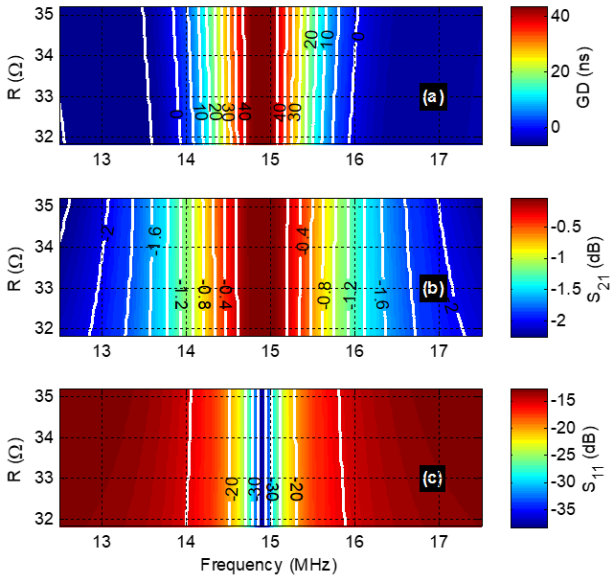

FIGURE 4. Mappings of (a) GD, (b) S_{21} and (c) S_{11} vs (f, R).

C. PARAMETRIC ANALYSIS OF INDUCTOR L

The sensitivity analysis of inductance L+/-5% of the LC series-network is discussed in the present paragraph. The inductor is varied linearly from 2.09 µH to 3.01 µH. Fig. 5 highlights the results represented by GD, S_{21} and S_{11} mappings in function of pair (frequency, inductor) or (f,L). The SB-NGD behavior is observed at any value of the inductor in the considered range of sensitivity analysis. It can be seen from Fig. 5(a), that the GD decreases when L increases. Furthermore, as depicted by Fig. 5(b) and Fig. 5(c), the transmission and the reflection coefficients decrease when L increases, respectively. Then, the center frequency decreases when L increases from 2.09 µH to 3.01 µH.

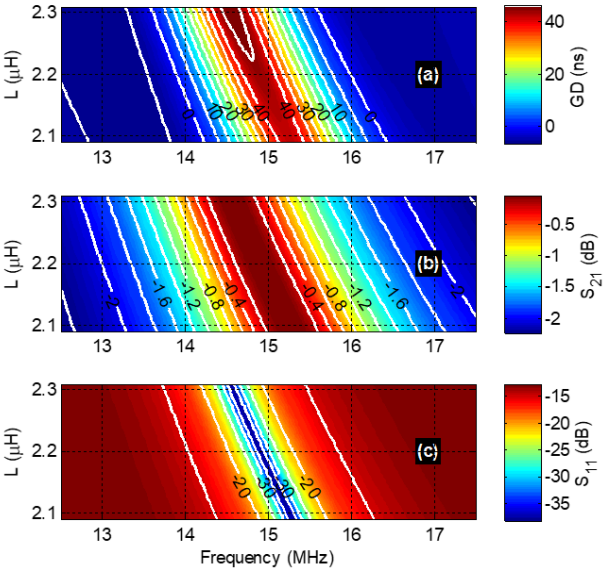

FIGURE 5. Mappings of (a) GD, (b) S_{21} and (c) S_{11} vs (f, L).

D. PARAMETRIC ANALYSIS OF CAPACITOR C

In this case, we are focusing on the influence of capacitor element on the SB-NGD response. Figs. 6 represent cartographies versus (f, C) of the sensitivity analysis with respect to capacitor C.

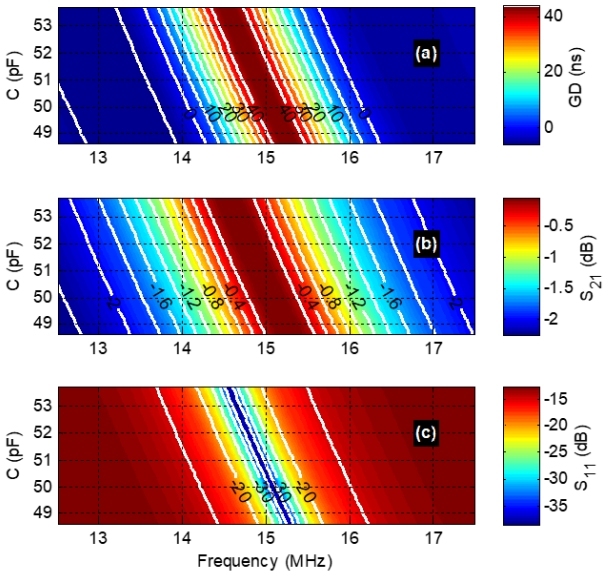

FIGURE 6. Mappings of (a) GD, (b) S_{21} and (c) S_{11} vs (f, C).

By varying this later, we can emphasize that the considered LC-network circuit conserve its SB-NGD behavior. Furthermore, the mapping plots of GD, S_{21} and S_{11} present similar behaviors with increase of their absolute values when C+/-5% varies from 48.64 pF to 53.76 pF. Then, the capacitor C influences inversely the value of the center frequency.

E. DISCUSSION ON THE SB-NGD PARAMETRIC ANALYSIS RESULTS

The previous sensitivity analyses permit to emphasize about the SB-NGD response influence versus the individual variation of each resistive, inductive and capacitive components constituting our circuit topology. It was found how the SB-NGD responses is conserved and also the basic parameters as GD, S_{11} and S_{21} are slightly sensitive to the component variations. It is particularly important to note that in the considered range of variation, parallel resistance R influences significantly the SB-NGD parameters. Then, the linear variation of reactive components L and C affects monotonically the NGD center frequency shift.

The sensitivity analyses enable to choose the appropriate and nominal values of SB-NGD circuit as POC to perform the comparative study between the theory and simulation from well-known electronic designer engineer commercial tool.

To verify the feasibility of the developed SB-NGD theory, a validation study is examined in the following section.

V. VALIDATION OF THE LC-SERIES NETWORK SB-NGD BEHAVIOUR

The validation results of the SB-NGD circuit are investigated in the present section. A prototype of fabricated lumped circuit is described. Then, the experimental validation results based on comparison with MATLAB® analytical calculation and commercial tool simulation will be discussed.

A. SB-NGD PROTOTYPE AND EXPERIMENTAL SETUP DESCRIPTION

The relevance of the previously established S-parameter and GD models is verified by designing the POC of the passive circuit. Fig. 7(a) displays the schematic of the simulated circuit. The POC circuit was schematized as a two-port circuit constituted by a parallel resistor with an LC-series network. This circuit POC is designed in the schematic environment of the electronic and RF/microwave design simulator of the ADS® commercial tool from Keysight Technologies®. Fig. 7(b) represents the photograph of the fabricated prototype which was implemented on FR4 epoxy substrate.

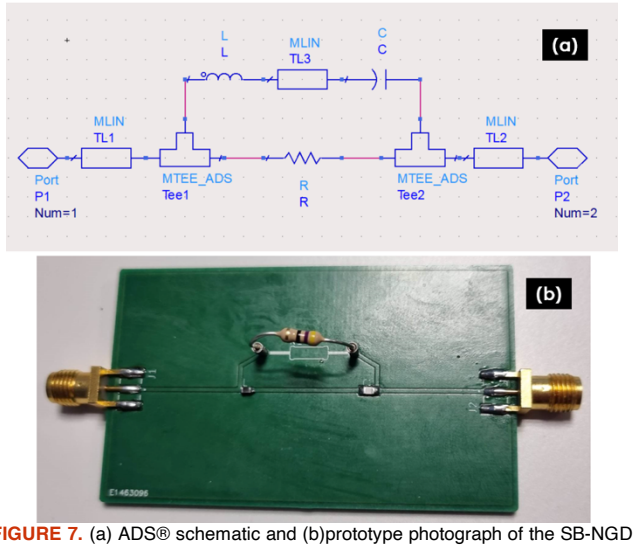

FIGURE 7. (a) ADS® schematic and (b)prototype photograph of the SB-NGD circuit POC.

The nominal values of SB-NGD circuit POC are addressed in Table IV. The lumped commercial components having +/-5% tolerances were considered for the fabricated prototype of the SB-NGD passive circuit under study.

TABLE IIIV. Nominal values of the fabricated SB-NGD circuit prototype components

Nature	Name	Value
Resistor	R	R_a=33 Ω R_b=47 Ω
Inductor	L	2.2 µH
Capacitor	C	51.2 pF

Fig. 8 shows the photograph of the prototyped SB-NGD circuit experimental setup by using vector network analyzer (VNA) referenced by MS2036C 10 kHz=20 GHz from ANRITSU®. The proposed experimental validation is based on comparison between the calculated and simulated S-parameters. The measurement tests were accomplished by the SOLT calibration.

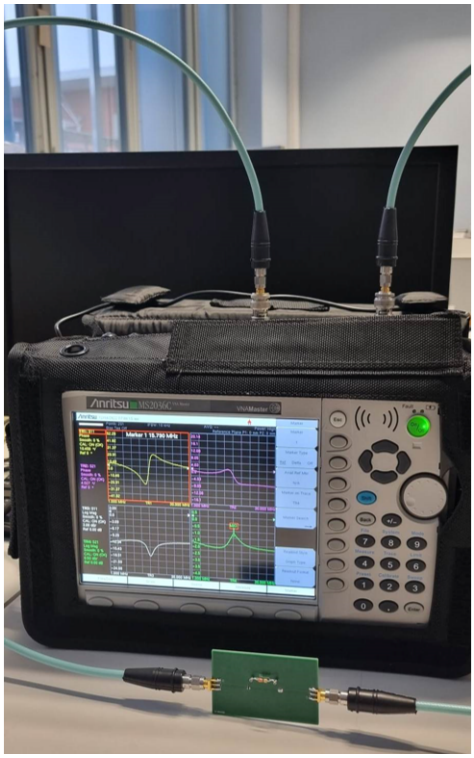

FIGURE 8. Comparisons between (a) magnitude and (b) phase of the transmission coefficients of the POC circuit from SPICE® simulation and the calculated model.

The obtained S-parameter simulation results were generated by using the well-known electronic designer engineer commercial tool. The next subsections are focused on the simulated and measured verification of the SB-NGD behavior.

B. VALIDATION RESULTS OF CALCULATED, SIMULATED AND MEASURED SB-NGD PROTOTYPED CIRCUIT

The S-parameter results of the SB-NGD circuit POC and prototype exposed by Figs. 7 were generated in the frequency domain from 10 MHz to 20 MHz. As expected, a good agreement between the theoretical, simulated and experimented S-parameters is observed over the considered frequency range. The comparisons between calculated (noticed by "Calc.", plotted in solid navy-blue curve) simulated (presented by "Simu.", plotted in dotted black curve) and measured (noticed by "Meas.", plotted in dashed red curve) and reflection are plotted in Fig. 9(a). It can be underlined that the reflection coefficients are all below -10 dB in the frequency band under consideration. Furthermore, the result showing the measured, simulated and calculated transmission coefficients is displayed in Fig. 9(b). The transmission coefficients with optimal frequency of about 13.55 MHz are literally better than -3 dB.

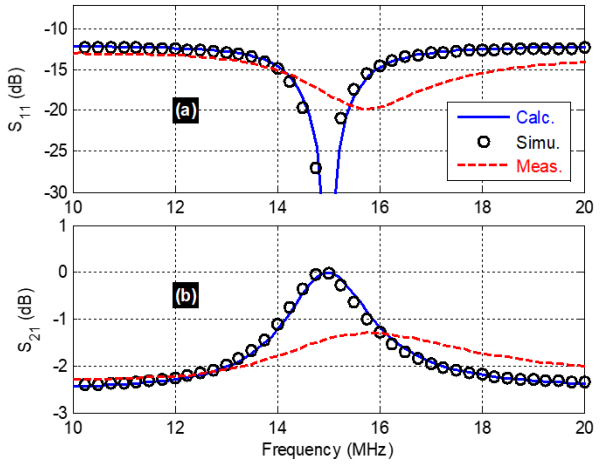

FIGURE 9. Comparisons between the calculated, simulated and measured (a) reflection and (b) transmission coefficients of the SB-NGD circuit POC shown in Figs. 7.

The comparison of SB-NGD circuit POC GDs displayed in Fig. 10. The modelled GD presented in this paragraph was computed from the analytical expression given in equation (16). It can be seen clearly that the topology of LC-network based circuit behaves as a SB-NGD function. The transmission coefficients are in good agreement despite the discrepancies of measured result due to the tolerance of used inductor and capacitor. The quality factor difference between the measurement and the predicted one is due to the parasitic and inaccuracies of the real components.

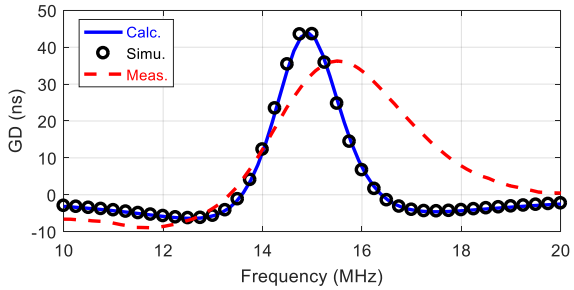

FIGURE 10. Comparison of calculated, simulated and measured GD responses of the SB-NGD prototype presented by Figs. 7.

TABLE IV. Calculated, simulated and measured SB-NGD parameters from the prototype shown by Figs. 4.

Name	f_0	$S_{11}(f_0)$	$S_{21}(f_0)$
Calculation	13.55 MHz	-0.001 dB	-50.45 dB
Simulation	13.4 MHz	-0.014 dB	-38.14 dB
Measurement	15.5 MHz	-1.35 dB	-19.6 dB

Table V summarizes the specifications of the SB-NGD responses. The obtained results of the present section enable to confirm concretely the feasibility of the SB-NGD function generation with the symmetric lumped circuit. The

most important remark from this study is that investigation on how to design a SB-NGD function is validated.

VI. CONCLUSION

An innovative SB-NGD theory of resonant passive RF circuit is developed. The SB-NGD study is originally based on the S-parameter modelling. First, the theoretical analysis of the general circuit assumed as a two-port circuit is introduced. Then, the basic specifications of the SB-NGD ideal responses are defined. The theoretical investigation is established with a passive and symmetric circuit constituted by an LC-series network. Afterwards, considerable sensitivity analyses with respect to the resistive and reactive components constituting our SB-NGD topology are performed. The proposed circuit SB-NGD circuit theory is validated by comparison between the calculated, simulated and measured circuit POC and prototype. As expected, the SB-NGD behavioral results are in very good agreement. The obtained results enable to confirm the effectiveness of the theoretical modelling for predicting the SB-NGD topology responses.

The NGD circuit engineering has very promising and wide future application. The NGD circuits are very good candidates for the development of future electronic and communication components, devices and systems. As non-exhaustively examples of preliminary work on NGD circuit Radio system:

- RF signal delay compensation in the communication system [3];
- RF and microwave signal integrity improvement [5];
- And design of negligible delay broadband BP-NGD phase shifter [7, 8].

REFERENCES

[1] J.-K. Xiao, Q.-F. Wang and J.-G. Ma, "Negative Group Circuits and Applications: Feedforward Amplifiers, Phased-Array Antennas, Constant Phase Shifters, Non-Foster Elements, Interconnection Equalization, and Power Dividers," IEEE Microw. Mag, vol. 22, no. 2, pp. 16-32, Feb 2021.

[2] C. D. Broomfield and J. K. A. Everard, "Broadband Negative Group Delay Networks for Compensation of Oscillators, Filters and Communication Systems," Electron. Lett., vol. 36, no. 23, pp. 1931-1933, Nov. 2000.

[3] B. Ravelo, S. Lalléchère, A. Thakur, A. Saini and P. Thakur, "Theory and circuit modelling of baseband and modulated signal delay compensations with low- and band-pass NGD effects," Int. J. Electron. Commun., vol. 70, no. 9, pp. 1122–1127, Sep. 2016.

[4] T. Shao, Z. Wang, S. Fang, H. Liu and Z. N. Chen, "A group-delay-compensation admittance inverter for full-passband self-equalization of linear-phase band-pass filter," Int. J. Electron. Commun., vol. 123, 153297, Aug. 2020.

[5] B. Ravelo, "Recovery of Microwave-Digital Signal Integrity with NGD Circuits," Photonics and Optoelectronics (P&O), vol. 2, no. 1, pp. 8-16, Jan. 2013.

[6] B. Ravelo, S. Ngoho, G. Fontgalland, L. Rajaoarisoa, W. Rahajandraibe, R. Vauché, Z. Xu, F. Wan, J. Ge, and S. Lalléchère, "Original Theory of NGD Low Pass-High Pass Composite Function for Designing Inductorless BP NGD Lumped Circuit," IEEE Access, vol. 8, pp. 192951-192964, Oct. 2020.

[7] B. Ravelo, "Distributed NGD active circuit for RF-microwave communication," Int. J. Electron. Commun., vol. 68, no. 4, pp. 282-290, Apr. 2014.

[8] J. Nebhen and B. Ravelo, "Innovative microwave design of frequency-independent passive phase shifter with LCL-network and bandpass NGD circuit," Progress In Electromagnetics Research (PIER) C, vol. 109, pp. 187–203, Feb. 2021.

[9] A. Mortazawi and W. Alomar, "Negative group delay circuit," United States Patent Application US20160093958, 2016. https://patents.google.com/patent/US20160093958A1/en.

[10] M. Zhu and C.-T. M. Wu, "Reconfigurable Series Feed Network for Squint-free Antenna Beamforming Using Distributed Amplifier-Based Negative Group Delay Circuit," Proc. 2019 49th European Microwave Conference (EuMC), Paris, France, pp. 256-259, Oct. 2019.

[11] H. Mirzaei and G. V. Eleftheriades, "Realizing non-Foster reactive elements using negative-group-delay networks," IEEE Trans. Microw. Theory Techn., vol. 61, no. 12, pp. 4322-4332, Dec. 2013.

[12] N. Au and C. Seo, "Novel design of a 2.1-2.9 GHz negative capacitance using a passive non-Foster circuit," IEICE Electron. Express, vol. 14, no. 1, pp. 1-6, Jan. 2017.

[13] Y. Meng, Z.Wang, S.-J. Fang, and H. Liu, "A Tri-Band Negative Group Delay Circuit for Multiband Wireless Applications," Progress In Electromagnetics Research C, vol. 108, pp. 159-169, Jan. 2021.

[14] B. Ségard and B. Macke, "Observation of Negative Velocity Pulse Propagation," Phys. Lett. A, vol. 109, no. 5, pp. 213-216, May 1985.

[15] Macke, B. and B. Ségard, "Propagation of light-pulses at a negative group-velocity," Eur. Phys. J. D, vol. 23, pp. 125–141, Apr. 2003.

[16] Munday, J. N. and W. M. Robertson, "Observation of Negative Group Delays within a Coaxial Photonic Crystal Using an Impulse Response Method," Optics Communications, vol. 273, no. 1, 2007, pp. 32-36.

[17] L. Markley and G. V. Eleftheriades, "Quad-Band Negative-Refractive-Index Transmission-Line Unit Cell with Reduced Group Delay," Electronics Letters, vol. 46, no. 17, pp. 1206-1208, Aug. 2010.

[18] G. Monti and L. Tarricone, "Negative Group Velocity in a Split Ring Resonator-Coupled Microstrip Line," Progress In Electromagnetics Research, vol. 94, pp. 33-47, Jul. 2009.

[19] J. J. Barroso, J. E. B. Oliveira, O. L. Coutinho and U. C. Hasar, "Negative group velocity in resistive lossy left-handed transmission lines," IET Microwaves, Antennas & Propagation, vol. 11, no. 15, pp. 2235-2240, Oct. 2017.

[20] Y. Kayano and H. Inoue, "Embedded F-SIR Type Transmission Line with Open-Stub for Negative Group Delay Characteristic," IEICE Trans. Electron., vol. E99-C, no. 9, pp. 1023–1026, Oct. 2016.

[21] G. Liu and J. Xu, "Compact transmission-type negative group delay circuit with low attenuation," Electronics Letters, vol. 53, no. 7, pp. 476-478, March 2017.

[22] G. Chaudhary and Y. Jeong, "Tunable center frequency negative group delay filter using coupling matrix approach," IEEE Microwave Wireless Component Letters, vol. 27, no. 1, pp. 37-39, Jan. 2017.

[23] T. Shao, Z. Wang, S. Fang, H. Liu, and S. Fu, "A compact transmission line self-matched negative group delay microwave circuit," IEEE Access, vol. 5, no. 1, pp. 22836-22843, Oct. 2017.

[24] T. Shao, S. Fang, Z. Wang and H. Liu, "A Compact Dual-Band Negative Group Delay Microwave Circuit," Radio Engineering, vol. 27, no. 4, pp. 1070-1076, Dec. 2018.

[25] L.-F. Qiu, L.-S. Wu, W.-Y. Yin, and J.-F. Mao, "Absorptive bandstop filter with prescribed negative group delay and bandwidth," IEEE Microw. Wireless Compon. Lett., vol. 27, no. 7, pp. 639-641, Jul. 2017.

[26] Z. Wang, Y. Cao, T. Shao, S. Fang and Y. Liu, "A Negative Group Delay Microwave Circuit Based on Signal Interference Techniques," IEEE Microw. Wireless Compon. Lett., vol. 28, no. 4, pp. 290-292, Apr. 2018.

[27] M. Kandic, and G. E. Bridges, "Asymptotic limits of negative group delay in active resonator-based distributed circuits," IEEE Trans. CAS I: Regular Papers, vol. 58, no. 8, pp. 1727-1735, Aug. 2011.

[28] B. Ravelo, "Similitude between the NGD function and filter gain behaviours," Int. J. Circ. Theor. Appl., vol. 42, no. 10, pp. 1016-1032, Oct. 2014.
[29] B. Ravelo, "High-Pass Negative Group Delay RC-Network Impedance," IEEE Trans. CAS II: Express Briefs, vol. 64, no. 9, 1052-1056, Sep 2017.
[30] B. Ravelo, "First-order low-pass negative group delay passive topology," Electronics Letters, vol. 52, no. 2, pp. 124–126, Jan. 2016.
[31] R. Randriatsiferana, Y. Gan, F. Wan, W. Rahajandraibe, R. Vauché, N. M. Murad and B. Ravelo, "Study and Experimentation of a 6-dB Attenuation Low-Pass NGD Circuit," Analog. Integr. Circ. Sig. Process., vol. 110, pp. 1-14, Jan. 2022.
[32] B. Ravelo, "On the low-pass, high-pass, bandpass and stop-band NGD RF passive circuits," URSI Radio Science Bulletin, vol. 2017, no. 363, pp. 10-27, Dec 2017.
[33] F. Wan, X. Huang, K. Gorshkov, B. Tishchuk, X. Hu, G. Chan, F. E. Sahoa, S. Baccar, M. Guerin, W. Rahajandraibe and B. Ravelo, "High-pass NGD characterization of resistive-inductive network based low-frequency circuit," COMPEL - The International Journal for Computation and Mathematics in Electrical and Electronic Engineering, vol. 40, no. 5, pp. 1032-1049, Oct. 2021.
[34] S. Ngoho, Y. C. Mombo Boussougou, S. S. Yazdani, Y. Dong, N. M. Murad, S. Lalléchère, W. Rahajandraibe and B. Ravelo, "Design and modelling of ladder-shape topology generating bandpass NGD function," Progress In Electromagnetics Research (PIER) C, vol. 115, pp. 145-160, Sep. 2021.
[35] E. J. R. Sambatra, S. Ngoho, F. Haddad, M. Guerin, G. Fontgalland, W. Rahajandraibe, and B. Ravelo, "Electrothermal Analyses of Bandpass NGD RLC-Network Topologies," Advanced Electromagnetics, vol. 12, no. 1, pp. 77–86, 2023.
[36] M. Guerin, Y. Liu, A. Douyère, G. Chan, F. Wan, S. Lalléchère, W. Rahajandraibe, and B. Ravelo, "Design and Synthesis of Inductorless Passive Cell Operating as Stop-Band Negative Group Delay Function," IEEE Access, vol. 9, no. 1, pp. 100141-100153, July 2021
[37] S. Fenni, F. Haddad, K. Gorshkov, B. Tishchuk, A. Jaomiary, F. Marty, G. Chan, M. Guerin, W. Rahajandraibe and B. Ravelo, "AC low-frequency characterization of stop-band negative group delay circuit," Progress In Electromagnetics Research (PIER) C, vol. 115, pp. 261-276, 2021.